Calculation and Error Analysis of a Digital Elevation Model of Hofsjökull, Iceland from SAR Interferometry

Jonathan S. Barton
General Sciences Corporation
NASA/Goddard Space Flight Center
Hydrological Sciences Branch, Code 974
Greenbelt, MD 20771
(301) 286-4738
Jonathan.S.Barton.1@gsfc.nasa.gov

Dorothy K. Hall
NASA/Goddard Space Flight Center
Hydrological Sciences Branch, Code 974
Greenbelt, MD 20771

Oddur Sigurðsson
Orkustofnun (National Energy Authority)
Vatnamælingar (Hydrological Service)
Grensásvegi 9, IS-108 Reykjavík, Iceland

Richard S. Williams, Jr.
USGS/Woods Hole Field Center
Woods Hole, MA 02543-1598

Laurence C. Smith
Department of Geography
University of California at Los Angeles
Los Angeles, CA 90095-1524

James B. Garvin
NASA/Goddard Space Flight Center
Geodynamics Branch, Code 921
Greenbelt, MD 20771

ABSTRACT

Two ascending European Space Agency (ESA) Earth Resources Satellites (ERS) -1/-2 tandem-mode, synthetic aperture radar (SAR) pairs are used to calculate the surface elevation of Hofsjökull, an ice cap in central Iceland. The motion component of the interferometric phase is calculated using the 30 arc-second resolution USGS GTOPO30 global digital elevation product and one of the ERS tandem pairs. The topography is then derived by subtracting the motion component from the other tandem pair. In order to assess the accuracy of the resultant digital elevation model (DEM), a geodetic airborne laser-altimetry swath is compared with the elevations derived from the interferometry. The DEM is also compared with elevations derived from a digitized topographic map of the ice cap from the University of Iceland Science Institute. Results show that low temporal correlation is a significant problem for the application of interferometry to small, low-elevation ice caps, even over a one-day repeat interval, and especially at the higher elevations. Results also show that an uncompensated error in the phase, ramping from northwest to southeast, present after tying the DEM to ground-control points, has resulted in a systematic error across the DEM.

Keywords: Synthetic Aperture Radar, Interferometry, Digital Elevation Model, Hofsjökull, topography

INTRODUCTION

Obtaining accurate topographic information of glaciers is extremely important. This is particularly true for remote sensing studies of glaciers, where the local slopes of the surface can have significant effects on the spectral signature. In synthetic aperture radar (SAR) studies of glaciers, the backscattering properties have been used to classify zones of similar signature (Fahnestock *et al.* 1993; Forster *et al.* 1996; Smith *et al.* 1997; Hall *et al.* submitted). Given the dependence of radar backscatter on topography, knowledge of the scattering surface could improve the estimation of the location of these zones.

Hofsjökull, an ice cap in central Iceland is the third largest ice cap in the country. Its location at a low elevation (< 2000m) for its size (area: 923km^2; volume: 208km^3) and geographic position just south of the Arctic Circle make it sensitive to changes in regional climate.

Existing topographic data for Hofsjökull are derived from aerial photogrammetry, such as the United States Geological Survey's GTOPO30 dataset, and from precision barometric altimetry acquired during radio-echosounding surveys (Björnsson 1988). Aerial photogrammetry, which requires the visual determination of elevation using contrast between overlapping vertical aerial photographs or satellite images, is not accurate over snow-covered glaciers. Such areas appear as

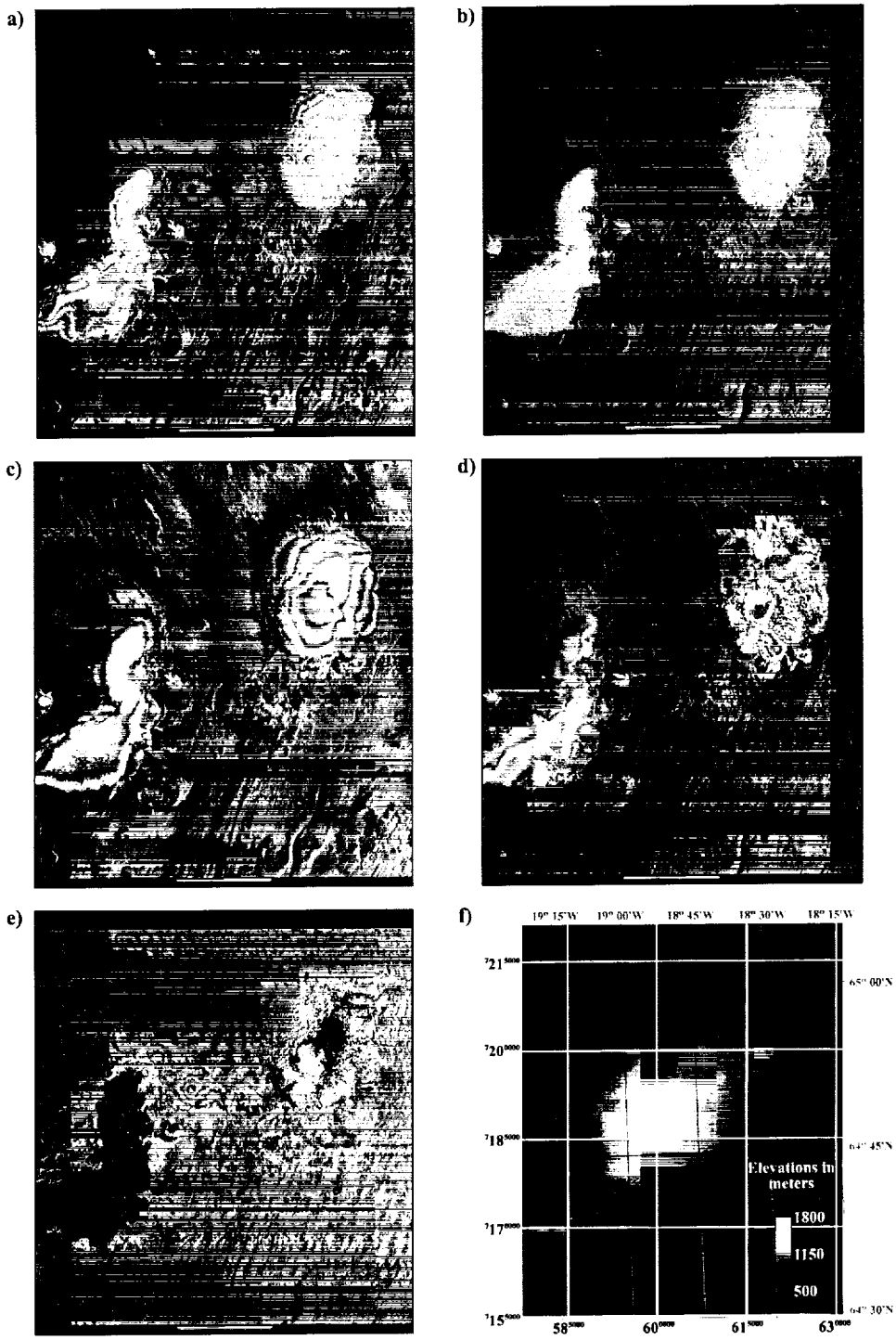

Plate 1. a) Flat-Earth-corrected interferogram created from the 2 January and 3 January 1996 SAR scenes. **b)** Flat-Earth-corrected interferogram created from the 6 February and 7 February 1996 SAR scenes. **c)** Synthetic interferogram created from the GTOPO30 DEM in the same orbit geometry as (a). **d)** Motion-only interferogram created by subtracting the topography-only interferogram (c) from the January motion+topography interferogram (a). **e)** Topography-only interferogram created by subtracting the motion-only interferogram (d) from the February motion+topography interfero-gram (b). Areas that were masked out of the unwrapping process because of low correlation (< 10%) are shown in black. **f)** Digital elevation model (DEM) created from the topography-only in-terferogram (e). The DEM is presented in the UTM (Zone 27) coordinate system. Elevations are relative to local mean sea-level. Maximum elevation is 1827m and minimum is 624m. The hori-zontal resolution is 16m x 39m and it is posted at a 12.5 m interval. Please see http://hydro4.gsfc.nasa.gov/STAFF/BartonJS/ESC/figures.html for color figures

monotonous areas of high reflectivity, with extremely low contrast. Snow-covered surfaces on satellite images, because of their high reflectivity, frequently exceed the dynamic range of radiometric sensitivity of detectors used in imaging sensors. Determination of elevation contours on stereoscopic images is therefore impossible under such a situation.

In 1983, ice-surface elevation and the bedrock below Hofsjökull were measured using precision barometric altimetry and radio-echosounding from a surface sledge. Ice thickness was measured at about 42,000 points, and the ice-surface was measured at about 30,000 points (Björnsson 1988). This methodology is more precise than aerial or satellite photogrammetry, but its low horizontal spatial resolution (average horizontal spatial resolution of 360m) renders it less than desirable for most remote-sensing studies.

Interferometric SAR (InSAR) has been shown to map high-resolution topography to within 5 m and displacements of the Earth's surface to sub-centimeter accuracy (Allen 1995). In particular, by measuring the phase differences between two temporally separated, coregistered images, InSAR has been used to make digital elevation models of several areas on the Earth, and to measure ice-sheet velocity in Greenland, Antarctica and alpine environments (Zebker and Goldstein 1986; Joughin 1995; Goldstein *et al.* 1993; Rignot *et al.* 1995; Mattar *et al.* 1998).

MEASUREMENTS

In this paper, the European Space Agency (ESA) Earth Resources Satellite (ERS) tandem datasets that were used in the production of the digital elevation model (DEM) are described along with the processing procedures used in the interferogram calculation. The process is similar to that detailed in Gabriel *et al.* (1989) and in Joughin (1995), so its description will not be repeated in detail. Finally, we analyze the accuracy of the InSAR DEM by comparing it to a geodetic airborne laser-altimetry swath, and to a ground survey-based topographic map.

Four ERS 1 and 2 (two each) single-look complex synthetic aperture radar images are produced from raw data obtained from the ESA United Kingdom and German Processing and Archiving Facilities using the Gamma Remote Sensing Modular SAR Processor (MSP) (Table 1).

Table 1. Radar scene descriptions

ERS	Orbit	Frame	Date	B_n (m)
1	23086	2295	02-Jan-96	88
2	03685	2295	03-Jan-96	
1	24859	2295	06-Feb-96	209
2	04186	2295	07-Feb-96	

Interferogram Generation

The first step in interferogram generation is for each pair of single-look complex (SLC) images to be coregistered to $^1/_{10}{}^{th}$ pixel accuracy (Zebker *et al.* 1994). This is followed by an estimation of the perpendicular baseline from the precision-orbit information provided by ESA. This estimate is then used to filter the range and azimuth spectra to maximize coherence after the method of Gatelli *et al.* (1994). Each pair is then cross-correlated, and multilook averaging over 2 pixels in range and 10 pixels in azimuth is performed to increase phase coherence. The azimuth and phase trends due to a flat Earth are then removed, producing two flattened interferograms (Plate 1a, Plate 1b), with the perpendicular baselines (B_n) given in meters in Table 1. This was done using the Gamma Remote Sensing Interferometric SAR Processor (ISP). The correlation was calculated for each of the interferograms using a five pixel by five pixel linearly weighted boxcar-averaging window (Figure 1a, Figure 1b). It is significant to note that while the correlation off of the glacier was frequently greater than 90 percent, the correlation on the glacier itself was very rarely greater than 65 percent, and at higher elevations, the correlation was for the most part below 15 percent.

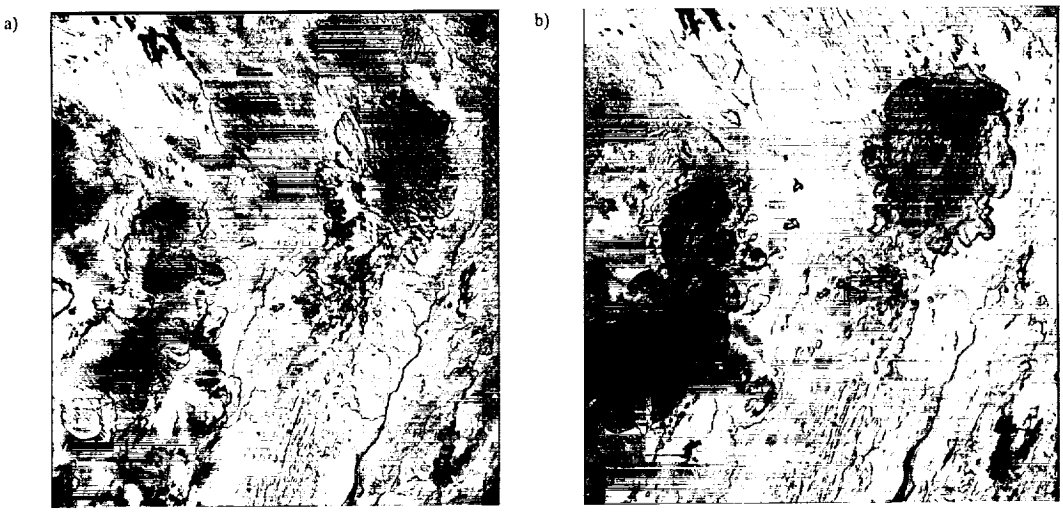

Figure 1. Correlation maps for the **a)** January and **b)** February interferograms. Note the very low correlation on the higher elevations of Hofsjökull in both maps.

The decorrelation on the higher elevations of the glacier presents a difficulty for the DEM generation. Joughin (1995) gives an excellent description of the factors that contribute to decorrelation, and many of these could be the controlling factor in the extreme decorrelation seen in Figure 1. Thermal decorrelation is constant across an interferogram, and is determined by the signal-to-noise ratio of the sensor; similarly, a misregistration between the scenes would produce decorrelation across the entire image, not just on the ice cap. Baseline decorrelation is minimal at these baselines (< 210m); it would also produce a distributed pattern. An assumed maximum penetration of about 10m at the highest elevations suggests that the volume scattering correlation coefficient is not significant at these baselines. All four of the scenes were processed using the same parameters; this should eliminate any mismatch decorrelation. Therefore, temporal decorrelation must be the dominant factor in limiting the accurate determination of surface elevation over parts of the ice cap, especially at higher elevations.

There is a variety of mechanisms that could cause this type of decorrelation. One of the most important features of the decorrelation is that its location does not follow similar patterns in the two correlation maps. This suggests that glacier motion is not the primary cause, because the motion should be nearly the same during the winter months. Another possibility is that blowing snow changes the surface properties of the ice cap significantly enough to influence the phase through the surface and volume scattering. A third mechanism is that following storms, which preceded the first image in January by five days and in February by two days, ongoing compaction of the snow cover produces different scattering paths during volume scattering, producing decorrelation. This mechanism corresponds best with the decrease in correlation with increase in elevation, because during a storm the amount of snow accumulation would be greater at higher elevations because of the orographic effect on precipitation.

Removing the Motion Signal

Because the glacier surface moves on the order of $10 cm \cdot d^{-1}$ at the equilibrium line, it is necessary to remove the motion of the surface in the line of sight of the radar sensor to isolate the topography component of the phase. The motion of the surface is determined using the method of Joughin *et al.* (1995), who applied the method of Massonnet *et al.* (1993) to glaciers, by removing the large-scale topography from the January interferogram. The topographic component of the January interferogram is modeled using the 30 arc-second resolution USGS GTOPO30 global DEM (derived from degraded Level 1 digital terrain elevation data (DTED) based on National Intelligence Mapping Agency (NIMA) Series 1501, 1:250,000-scale map of Hofsjökull and environs (sheet NQ 27,28-14) which are in turn based on A.M.S. Series C762 1:50,000-scale maps) and the

Gamma Remote Sensing Differential InSAR Processor (DIFF) (Alsdorf and Smith in press). The resultant synthetic interferogram (Plate 1c) is subtracted from the January interferogram using the DIFF. The component of the phase due to motion in the January interferogram is shown in Plate 1d. The 30 arc-second resolution (about 0.9 km x 0.4 km at 64° 45' N latitude) of the DEM allows some phase error to be introduced into the interferogram due to fine topographic features.

At the relatively short perpendicular baseline of B_n=88m of the January pair, a change in phase of 2π radians corresponds to vertical relief of approximately 110m. This is greater than most of the anticipated fine resolution relief, except in localized areas around nunataks, which may be omitted from the low-resolution DEM. Because the phase variation seen on the interferogram far exceeds 2π radians, it can be assumed that the residual topography causes minimal phase effects on the interferogram.

In order to determine the phase due to the topography field as sensed by the SAR system, the motion calculated from the January interferogram and the GTOPO30 DEM was assumed to be constant during the deep winter months, and therefore the phase due to the motion in January should be the same as the phase due to the motion in February. Subtracting the phase due to the motion from the February interferogram yields an interferogram of entirely topographic phase effects, assuming that atmospheric interference is minimal (Plate 1e.). Meteorological data for the Hveravellir meteorological station, located nearly in the center of the radar scenes, indicates that no storms passed through on any of the four days imaged, suggesting that, to a certain level, this assumption is valid. This method is similar to that used by Kwok & Fahnestock (1996).

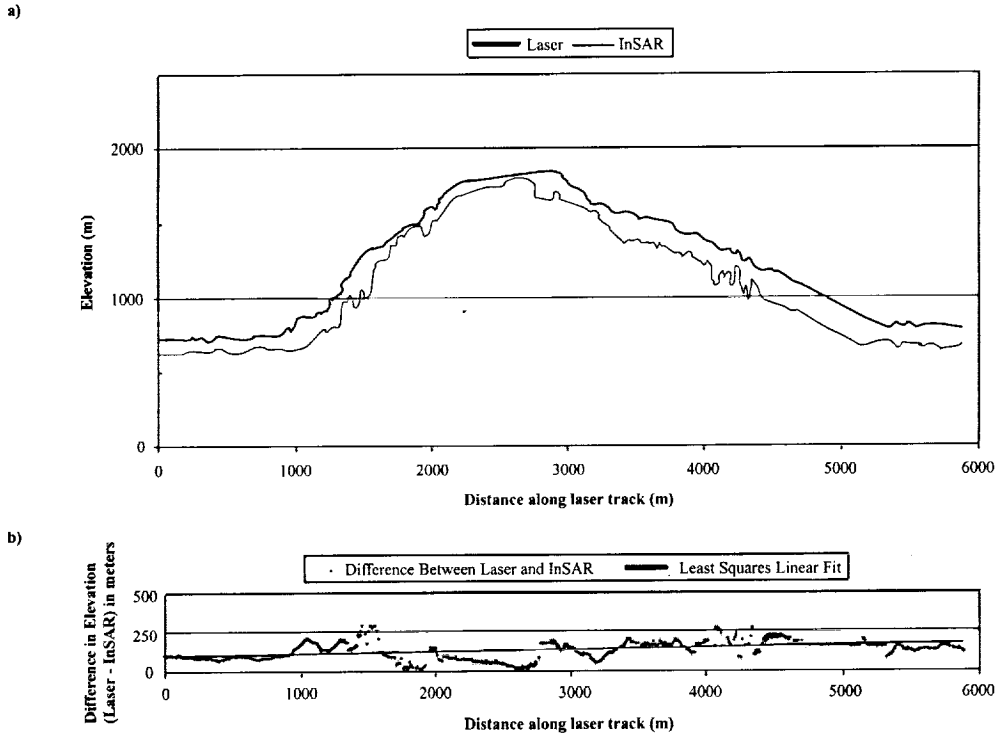

Figure 2. Comparison of the geodetic laser altimetry swath (70m posted subset) with the same locations from the InSAR DEM; **a)** shows the elevations given by each instrument, and **b)** shows the difference between the two.

Phase Unwrapping and DEM Generation

After masking of low (< 10%) correlation areas, the phase was filtered to reduce phase noise and unwrapped, after the method described in Goldstein *et al.* (1988). Because of the limitations on baseline estimation from the ESA orbital data, which have an accuracy of about 30cm and allow global height errors of the order of 1km, ground-control points are required to use the much more accurate relative measurements (Zebker *et al.* 1994.). Twenty ground-control points were taken from 1:50,000-scale (DMA, Series C761) maps. None of the ground-control points selected was located on the glacier surface, because of topographic inaccuracies in the maps arising from low

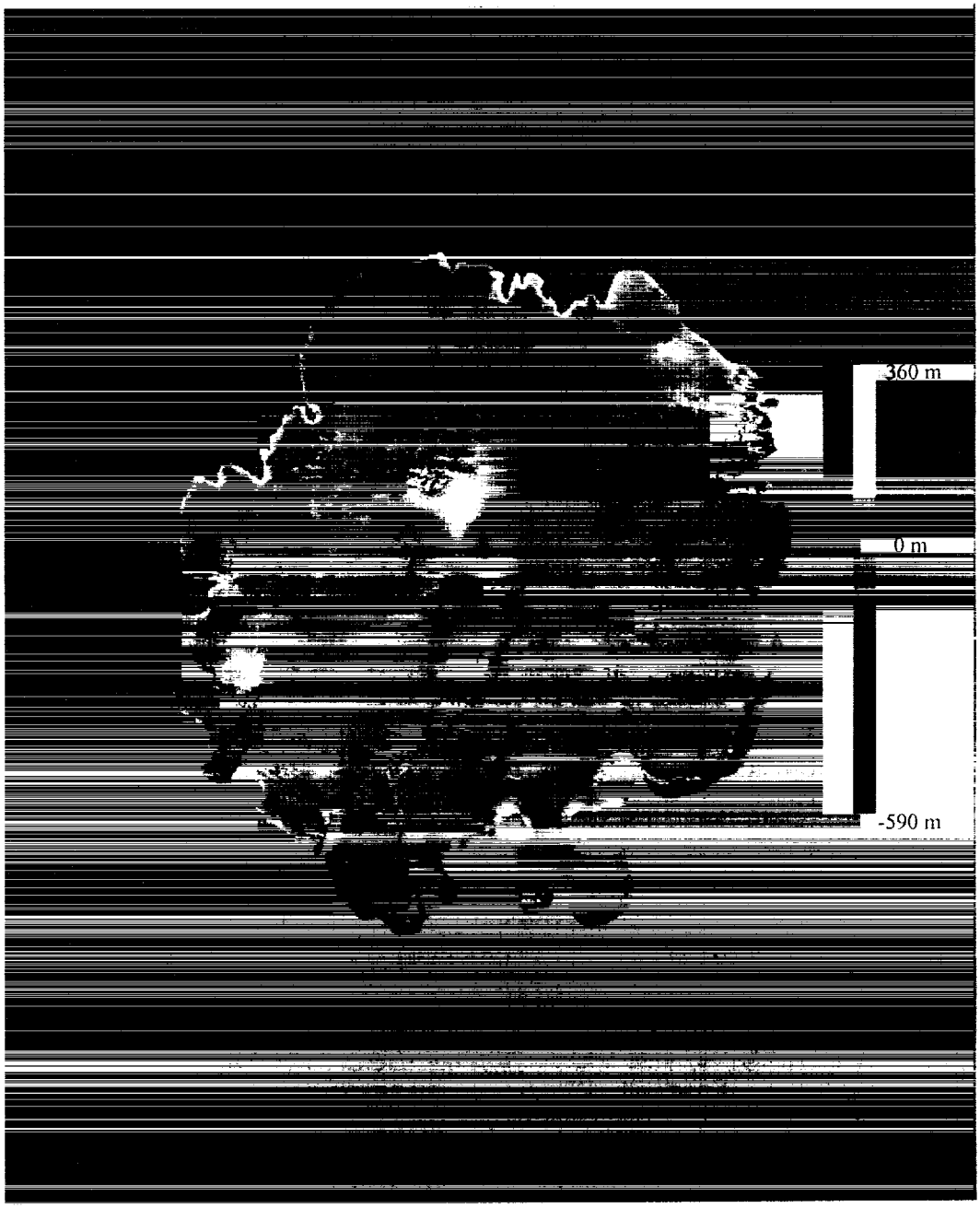

Figure 3. Comparison of the InSAR DEM with the rasterized elevation map from the University of Iceland Science Institute. The values shown are the InSAR elevations minus the University of Ice-land elevations.

image contrast on the glacier surface above the snowline. Because the elevations on these maps are relative to local sea level, the global shifts calculated by the processor utilizing the ground-control points force the interferometric DEM to be relative to local sea level as well. After baseline reestimation, a DEM was created, following the method of Madsen *et al.* (1993), and geolocated using the elevations and the satellite state-vectors. In areas where the low-correlation made phase unwrapping impossible, data from the GTOPO30 DEM was substituted as a first-order approximation of the surface (Plate 1f).

ERROR ANALYSIS AND FUTURE WORK

In order to assess the absolute accuracy of the resulting DEM, a 70m posting of a west-to-east geodetic airborne laser altimetry (GALA) swath (10cm vertical accuracy), obtained by a NASA p-3 survey aircraft in July 1997, was compared to the corresponding swath across the derived DEM (Figure 2). There is a significant systematic difference between the two, indicating an error in the interferometric DEM. The source of the error is most likely baseline estimation error, which manifests itself in the southeast-northwest trending phase ramp of Plate 1d. There are highly regular fringes indicating up to 14cm of motion (per day) of the surface of the ground surrounding the glacier surface. The local deviations from the planar tilt, which is caused by the baseline errors, are best explained by areas of low (< 20%) correlation, and hence very low signal-to-noise ratio.

In order to assess the relative accuracy of the DEM against existing elevation data, it was compared to a rasterization of a digitized topographic map from the University of Iceland Science Institute. Because of the absence of precise cartographic parameters for the Science Institute map, the registration of the two DEMs was not completely accurate. However, since, at the resolution of the rasterization (100 m), the ice cap is very smooth, this misregistration yields small errors on the ice cap itself, and large errors only near the edges.

The spatial distribution of errors is shown in Figure 3. The large positive errors near the perimeter of the ice cap are caused by misregistration effects, and the large negative errors in the northeastern corner of the ice cap are due to layover and poor correlation in the radar images. However, even with these localized regions of high error, the 95% bracket falls at about ±100m. On the difference map, the ramp observed in the laser altimetry plots is again observed. The southeasterly part of the glacier shows predominantly negative differences, while the northwesterly part shows predominantly positive differences; this is consistent with the phase ramp seen in the motion interferogram.

It may be possible to correct for the effects of this phase ramp using additional data. Because the laser altimetry data are so accurate, a north-to-south line collected in July 1998 in addition to the west-to-east line mentioned above, could be used to warp the DEM to the GALA profiles.

CONCLUSIONS

It is possible to calculate accurate DEMs of small glacier surfaces with spaceborne radar interferometry, but global errors are difficult to eliminate. In order to remove phase ramps caused by inaccurate baseline estimation, independent, reliable geodetic information must be available for the determination of ground-control points.

Decorrelation, even over the one-day temporal separation of the tandem mission, can be a problem on some temperate glacier surfaces. This decorrelation may be explained, in part, by the compaction of recent snowfall or snow drifting. Unfortunately, during the tandem mission, there were no passes over Hofsjökull that resulted in high correlation over the entire surface. Thus for Hofsjökull and other ice caps, it is necessary to rely on additional datasets to augment the radar data to improve the global accuracy of the InSAR-derived surface elevations.

REFERENCES

Allen, C.T. 1995. "Interferometric synthetic aperture radar", *IEEE Geoscience and Remote Sensing Society Newsletter* **96**, 6-13.

Alsdorf, D.E. & L.C. Smith 1999. "Interferometric SAR observations of ice topography and velocity changes related to the 1996 Gjalp subglacial eruption, Iceland", accepted for publication to *International Journal of Remote Sensing*.

Bjornsson, H. 1988. *Hydrology of ice caps in the volcanic regions*, Vísindafélag Íslendinga, Reykjavík, 139 p.

Fahnestock, M., R. Bindschadler, R. Kwok, & K. Jezek 1993, "Greenland ice sheet surface properties and ice dynamics from ERS-1 synthetic aperture radar imagery", *Science* **262**, 1530-1534.

Forster, R., B.L. Isacks, & S. Das 1996. "Spaceborne imaging radar (SIR-C/X-SAR) reveals near-surface properties of the South Patagonian Icefield", *Journal of Geophysical Research* **101**(E10), 23169-23180.

Gabriel, A.K., R.M. Goldstein, & H.A. Zebker 1989. "Mapping small elevation changes over large areas: Differential radar inteferometry", *Journal of Geophysical Research* **94**(B7), 9183-9191.

Gatelli, F., A. Monti-Guarnieri, F. Parizzi, P. Pasquali, C. Prati, & F. Rocca 1994. "The wavenumber shift in SAR interferometry", *IEEE Transactions on Geoscience and Remote Sensing* **32**, 855-865.

Goldstein, R.M., H.A.Zebker, & C.L. Werner 1988, "Satellite radar interferometry: Two-dimensional phase unwrapping", *Radio Science* **23**, 713-720.

Goldstein, R.M., H. Engelhardt, B. Kamb, & R.M. Frolich 1993. "Satellite radar interferometry for monitoring ice sheet motion: Application to an Antarctic ice stream", *Science* **262**, 1525-1530.

Hall, D.K., R.S. Williams, Jr., J.S. Barton, O. Sigurðsson, L.C. Smith, J.B. Garvin 1999. "Evaluation of Remote Sensing Techniques to Measure Decadal-Scale Changes in the Mass Balance of Hofsjökull Ice Cap, Iceland", submitted for publication to Journal of Glaciology.

Joughin, I. 1995. *Estimation of Ice-Sheet Topography and Motion Using Interferometric Synthetic Aperture Radar*, Ph.D. Dissertation, Department of Electrical Engineering, University of Washington, 182 p.

Joughin, I.R., D.P. Winebrenner, & M.A. Fahnestock 1995. "Observations of ice-sheet motion in Greenland using satellite radar interferometry", *Geophysical Research Letters* **22**(5), 571-574.

Kwok, R., & M.A. Fahnestock 1996, "Ice sheet motion and topography from radar interferometry", *IEEE Transactions on Geoscience and Remote Sensing* **34**(1), 189-200.

Madsen, S.N., H.A. Zebker, & J.M. Martin 1993, "Topographic mapping using radar inteferometry: Processing Techniques", *IEEE Transactions on Geoscience and Remote Sensing* **31**(1), 246-256.

Massonnet, D., M. Rossi, C. Carmona, F. Adragna, G. Peltzer, K. Feigl, & T. Rabaute 1993. "The displacement field of the Landers earthquake mapped by radar inteferometry", *Nature* **364**, 138-142.

Mattar, K.E., P.W. Vachon, D. Geudtner, A.L. Gray, I.G. Cumming, & M. Brugman 1998. "Validation of alpine glacier velocity measurements using ERS tandem-mission SAR data", *IEEE Transactions on Geoscience and Remote Sensing* **36**(3), 974-984.

Rignot, E., K.C. Jezek, & H.G. Sohn 1995. "Ice flow dynamics of the Greenland ice sheet from SAR inteferometry", *Geophysical Research Letters* **22**(5), 575-578.

Smith, L.C., R.R. Forster, B.L. Isacks, & D.K. Hall 1997. "Seasonal climatic forcing of alpine glaciers revealed with orbital synthetic aperture radar", *Journal of Glaciology* **43**(145), 480-488.

Zebker, H.A. & R.M. Goldstein 1986. "Topographic mapping from interferometric synthetic aperture radar", *Journal of Geophysical Research* **91**(B5), 4993-4999.

Zebker, H.A., C.L. Werner, P.A. Rosen, & S. Hensley 1994. "Accuracy of topographic maps derived from ERS-1 interferometric radar", *IEEE Transactions on Geoscience and Remote Sensing* **32**(4), 823-836.